Polym. Bull. (2013) 70:403–417
DOI 10.1007/s00289-012-0799-6

ORIGINAL PAPER

Effect of SiO_2 and nanoclay on the properties of wood polymer nanocomposite

Biplab K. Deka · Tarun K. Maji

Received: 6 September 2011 / Revised: 18 April 2012 / Accepted: 16 June 2012 /
Published online: 23 June 2012

Abstract Wood polymer composite (WPC) were developed by using solution blended high density polyethylene, low density polyethylene, polypropylene, poly(vinyl chloride), *Phragmites karka* wood flour and polyethylene-*co*-glycidyl methacrylate. The effect of addition of nanoclay and SiO_2 on the properties of the composite was examined. X-ray diffractrometry and transmission electron microscopy were used to study the distribution of silicate layers and SiO_2 nanopowder in the composite. The improvement in miscibility among the polymers and WPC was studied by scanning electron microscopy. Fourier transform infrared spectroscopy study revealed the interaction between polymer, wood, clay and SiO_2. WPC treated with 3 wt% each of clay and SiO_2 showed an excellent improvement in mechanical properties, thermal and flame retarding properties. Water uptake of WPC was found to decrease on incorporation of nanoclay and SiO_2 in WPC.

Keywords Nanocomposites · Polymers · Nanoclay · Mechanical properties · Transmission electron microscopy

Introduction

During the last few decades, wood polymer composite (WPC) have emerged as an important family of green composite [1]. They are used in different outdoor, indoor applications like decking, railing, fencing, docks, landscaping timbers, and in a number of automobiles industries [2]. The composites reinforced with wood have shown a great grown due to the many advantages that they possess. Their processing

B. K. Deka · T. K. Maji (✉)
Department of Chemical Sciences, Tezpur University, Tezpur 784028, Assam, India
e-mail: tkm@tezu.ernet.in

is easy, economic, and ecological. They have relatively high strength and stiffness, low cost, low density, low CO_2 emission, biodegradability and renewable. Varieties of non conventional plant materials like Nal (*Phragmites karka*), a type of non conventional plant, is abundantly available in the forest of Assam, India. These are mostly utilized for fuel purposes or remain as bio wastes. Their uses for structural purposes are restricted due to their poor mechanical properties and dimensional stability. They can be made value added material for preparation of structural components by making composites with plastics materials. These composites will not only contribute to the economical growth but it can also reduce the amount of bio wastes. Sui et al. [3] has prepared WPC by using sunflower hull sanding dust (SHSD), a non conventional plant as reinforcing agent and PP as matrix.

Polypropylene (PP) [4], high density polyethylene (HDPE) [5], low density polyethylene (LDPE) [6], poly(vinyl chloride) (PVC) [7], are the most widely used plastics in large volume because of their versatile properties like light weight, resistance to breakage, low cost, ease of manufacture, fabrication and shaping. These materials can be used by combining with other materials, laminating or blending with other polymers to gain the benefit of their various attributes. The wastage arises from varieties of plastic articles in the form of garbage is a major environmental concern in recent days [8]. One of the ways to minimise the problem is by forming composites of waste plastics with wood. In order to improve the miscibility between hydrophobic polymers and hydrophilic wood flour (WF), compatibilizers are used. They act as a bridging agent between the two interfaces. Compatibilizers like glycidyl methacrylate, maleated PP have significantly improved the properties of the wood polymer composite [9, 10].

In the polymer composites, different types of filler are used for improving the thermal, mechanical, as well as other properties. Among them, clay is widely used as filler. The surface characteristics of nanopowders play a key role in their fundamental properties from phase transformation to reactivity. A dramatic increase in the interfacial area between fillers and polymer can significantly improve the properties of the polymer [11]. Different types of metal oxide nanoparticles such as SiO_2, TiO_2, ZnO, etc., are widely used for these purposes. These are non-toxic, stable and highly thermostable inorganic filler.

In polymer composite, SiO_2 nanopowder is one of the widely used filler. SiO_2 can enhance the mechanical as well as thermal properties of the composite. Polymer–SiO_2 composites have been explored as technological importance due to their potential applications in electrochromic windows, fuel cells, chemical separation, electrochemical sensing, and water treatment [12]. SiO_2 nanoparticles extensively increase the tensile and impact strength of epoxy nanocomposite [13]. In order to increase the hydrophobicity of the inorganic silica particles, the surface has been modified by different silane compound [14].

In this communication, we report the modification of SiO_2 by treatment with cetyl trimethyl ammonium bromide and study the effect of SiO_2 nanopowder along with nanoclay on various properties of composites based on wood, PE-*co*-GMA and polymer mixture of HDPE, LDPE, PP, and PVC.

Experimental

Materials

HDPE and LDPE (Grade: PE/20/TK/CN) were obtained by the courtesy of Plast Alloys India Ltd. (Harayana, India). PP homopolymer (Grade: H110MA, MFI 11 g/10 min), PVC (Grade: SPVC FS: 6701) were supplied by Reliance Industries Ltd. (Mumbai, India) and Finolex Industries Ltd. (Pune, India), respectively. The compatibilizer poly(ethylene-*co*-glycidyl methacrylate) (PE-*co*-GMA) (Otto chemicals, Mumbai, India), *N*-cetyl-*N*,*N*,*N*-trimethyl ammonium bromide (CTAB) (Central Drug house (P) Ltd, Delhi, India), nanomer (clay modified by 15–35 wt% octadecylamine and 0.5–5 wt% aminopropyltriethoxy silane) (Sigma-Aldrich, USA) and SiO_2 nanopowder (5–15 nm, 99.5 % trace metals basis) (Aldrich, China) were used as such received. A non-conventional wood, Nal (*P. karka*), was collected from local forest of Assam. Other reagents used were of analytical grade.

Preparation of wood samples

Nals (*P. karka*), a kind of soft wood, is available in the forest of Assam. It was collected and chopped into small strips. These were initially washed with 1 % soap solution followed by washing with 1 % NaOH solution and finally with cold water. The washed wood strips were oven dried at 100 ± 5 °C till the attainment of constant weight. These dried wood strips were grinded in a mixer, sieved at 60 mesh sizes and kept for subsequent uses.

Modification of SiO_2

Ten gram of SiO_2 was taken in a round bottom flask containing 1:1 ethanol–water mixture stirred at 80 °C for 12 h. 12 g of CTAB was taken in a beaker containing ethanol–water mixture and stirred at 80 °C for 3 h. This mixture was added slowly to the flask containing SiO_2 mixture under stirring condition. The stirring was continued for 6 h. The mixture was then filtered and washed with deionised water for several times. It was collected, dried in vacuum oven at 45 °C, grinded and stored in desiccator to avoid moisture absorption. CTAB-modified SiO_2 was dispersed in a flask containing xylene and kept for checking of any settling of particles. The dispersion of SiO_2 was found to be stable. This indicated that proper modification occurred.

Preparation of wood polymer nanocomposite

The minimum ratio of xylene and THF, at which a homogenous mixture of HDPE, LDPE, PP, and PVC was obtained, was optimized as 70:30. 6 g each of HDPE, LDPE, and PP (1:1:1) were added slowly to a flask containing 105 ml of xylene at room temperature. This was followed by the addition of the PE-*co*-GMA (5 wt%). The temperature of the flask was increased from room temperature to 130 °C in order to make a homogenous solution. Now, another solution containing 3 g of PVC

in 35 ml of tetrahydrofuran (THF) was prepared. The temperature of the polymer solution containing HDPE, LDPE, and PP was brought down to 120 °C. To this, PVC solution was added gradually and stirring was continued at 120 °C (approximately) for 1 h. A known quantity of nanomer (3 wt%) and CTAB-modified SiO_2 nanopowder (1–5 wt%) was dispersed in 10 ml of THF solution by sonication. This dispersed mixture was added gradually to the polymer solution under stirring condition. Oven-dried WF (40 wt%) was added slowly to this solution. The whole mixture was stirred for another 1 h. The mixture was transferred to a tray, dried and grinded. The composite sheets were obtained by the compression molding press (Santec, New Delhi) at 150 °C under a pressure of 80 MPa.

Polymer blend (HDPE + LDPE + PP + PVC), polymer blend/5 wt% PE-*co*-GMA and polymer blend/5 wt% PE-*co*-GMA/40 wt % wood were designated as PB, PB/G5, and PB/G5/W40. WPC filled with 3 wt% nanoclay and 1, 3, and 5 wt% SiO_2 were designated as PB/G5/W40/N3/S1, PB/G5/W40/N3/S3, and PB/G5/W40/N3/S5.

Measurements

X-ray diffraction (XRD)

The degree of nanoclay dispersion and SiO_2 distribution in the WPC were evaluated by X-ray diffraction (XRD) analysis. It was carried out in a Rigaku X-ray diffractometer (Miniflax, UK) using CuKα ($\lambda = 0.154$ nm) radiation at a scanning rate of 1°/min with an angle ranging from 2° to 70°.

Transmission electron microscopy (TEM)

The study of the dispersion of nanoclay and SiO_2 nanoparticles in WPCs was performed by using transmission electron microscope (JEM-100 CX II) at an accelerated voltage of 20–100 kV.

Scanning electron microscopy (SEM)

The compatibility among different polymers and morphological features of the WPC were studied by using scanning electron microscope (JEOL JSM-6390LV) at an accelerated voltage of 5–10 kV. Fractured surface of the samples, deposited on a brass holder and sputtered with platinum, were used for this study.

FTIR studies

FTIR spectra of WF, nanoclay, SiO_2 nanopowder, and WPC loaded with nanoclay and SiO_2 were recorded in FTIR spectrophotometer (Impact-410, Nicolet, USA) using KBr pellet.

Mechanical property

The tensile and flexural tests for polymer blend, PE-*co*-GMA treated polymer blend, and WPC loaded with different percentage of nanoclay and SiO_2 were carried out using Universal Testing Machine (Zwick, model Z010) at a crosshead speed of 10 mm/min at room temperature according to ASTM D-638 and D-790, respectively. Ten samples of each category were tested and their average values were reported.

Hardness

The hardness of the samples was measured according to ASTM D-2240 using a durometer (model RR12) and expressed as shore D hardness.

Thermal property

Thermal properties of polymer blend and the WPCs were measured in a thermogravimetric analyser (TGA) (TGA-50, shimadzu) at a heating rate of 10 °C/min up to 600 °C under nitrogen atmosphere.

Limiting oxygen index (LOI)

Limiting oxygen index (LOI) of the samples was measured by flammability tester (S.C. Dey Co., Kolkata) according to ASTM D-2863 method. The ratio of nitrogen and oxygen at which the samples continue to burn for at least 30 s were recorded.

$$\text{Limiting oxygen index (LOI)} = \text{Volume of } O_2/\text{Volume of } (O_2 + N_2) \times 100.$$

Water uptake test

WPC samples were cut into $2.5 \times 0.5 \times 2.5$ cm^3 for the test. Percentage water uptake was measured by submerging the samples in distilled water at room temperature (30 °C) for different time periods after conditioning at 65 % relative humidity and 30 °C and expressed according to the formulae below,

$$\text{Water uptake } (\%) = (W_s - W_1)/W_1 \times 100,$$

where W_s is the weight of the water saturated specimen, and W_1 is the weight of the oven-dried specimen.

Results and discussion

XRD results

XRD results of nanoclay, polymer-blend, SiO_2 and wood polymer composite loaded with clay (3 wt%), and different percentage of SiO_2 (1–5 wt%) are represented in

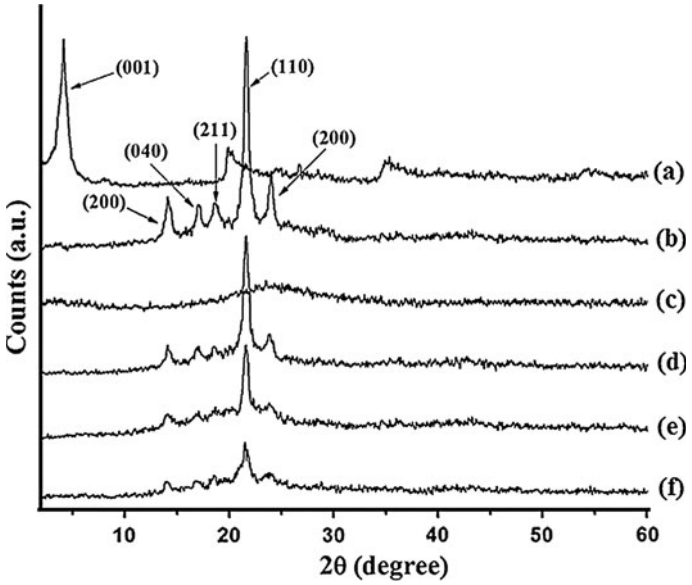

Fig. 1 X-ray diffraction of (*a*) nanoclay, (*b*) PB, (*c*) nano SiO_2, (*d*) PB/G5/W40/N3/S1, (*e*) PB/G5/W40/N3/S3, and (*f*) PB/G5/W40/N3/S5

Fig. 1. Organically modified nanoclay (curve a) shows the diffraction peak at $2\theta = 4.11°$ with a basal spacing of 2.15 nm. In the diffractrogram of polymer blend (curve b), the most prominent wide-angle XRD peaks appeared at $2\theta = 14.12$ (200), 17.06 (040), 18.64 (211), 21.62 (110), and 24.02 (200) were for crystalline portion of different polymers present in the blend [15–18]. Curve c shows a broad diffraction peak at $2\theta = 23.5°$ for the amorphous SiO_2 nanoparticles. Curves (d–f) represent the diffractrograms of WPC loaded with nanoclay (3 wt%) and different percentage of SiO_2 (1–5 wt%). The figures did not exhibit any characteristic peak of nanoclay. The exfoliation of silicate layers in the wood polymer matrix was the cause for disappearance of nanoclay diffraction peak. The crystalline peak intensity of the polymer blend appeared in the range of $2\theta = 14$–$25°$ was found to decrease with the increase in the level of incorporation of SiO_2 (1–5 wt%). Similar decrease in peak intensities of polymer and increase in peak intensity due to incorporation of TiO_2 was observed and reported by Mina et al. [15] while studying the XRD profile of PP/titanium dioxide composite. This suggested that the nanoclay layers were exfoliated and SiO_2 particles were dispersed in the wood polymer matrix.

TEM results

TEM micrographs of polymer blend loaded with compatibilizer, WPC and WPC loaded with nanoclay and different percentage of SiO_2 (1–5 wt%) are shown in Fig. 2. The silicate layers of nanoclay are represented by dark lines and the SiO_2 nanoparticles are presented by black spots in the figures. At lower percentage of SiO_2 loading (1–3 wt%), a good dispersion of clay and SiO_2 nanoparticles was

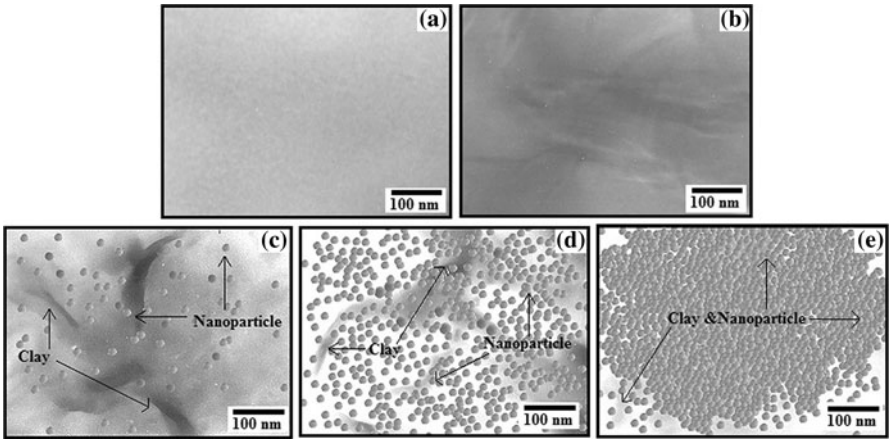

Fig. 2 TEM micrographs of (*a*) PB/G5, (*b*) PB/G5/W40, (*c*) PB/G5/W40/N3/S1, (*d*) PB/G5/W40/N3/S3, and (*e*) PB/G5/W40/N3/S5

observed. Na-MMT layers together with SiO_2 nanoparticles were found to disperse well in PMMA matrix as reported by Bao and Ma [19]. At higher percentage of SiO_2 (5 wt%) loading, an agglomeration of the nanoparticles was observed. The agglomeration occurred due to the surface interaction among the nanoparticles.

SEM results

Figure 3 shows the SEM micrographs of different fractured samples of PB, WPC and WPC loaded with nanoclay (3 wt%) and different percentage of SiO_2 (1–5 wt%) nanopowder. The polymers were found immiscible (Fig. 3a) at the first stage. But after the incorporation of compatibilizer, the miscibility among the

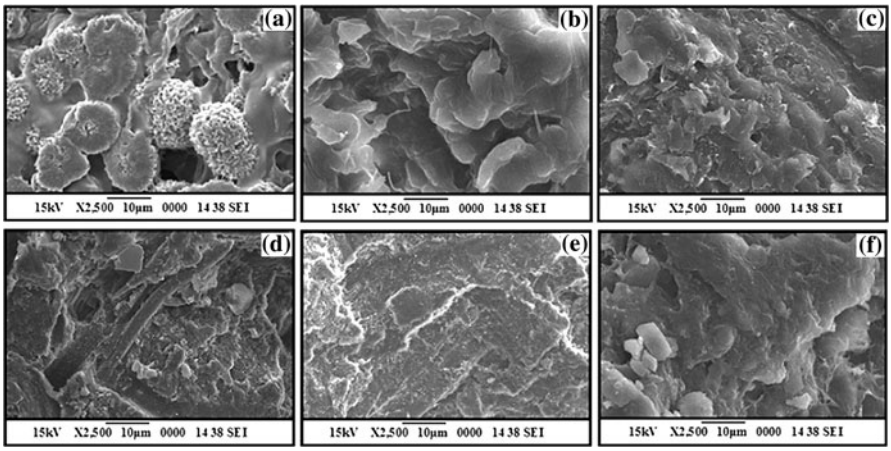

Fig. 3 SEM micrographs of (*a*) PB, (*b*) PB/G5, (*c*) PB/G5/W40, (*d*) PB/G5/W40/N3/S1, (*e*) PB/G5/W40/N3/S3, and (*f*) PB/G5/W40/N3/S5

polymers increased (Fig. 3b). The compatibilizer increased the interfacial adhesion among the polymers, and thereby improved the miscibility among them [20]. The addition of WF improved the smoothness of composite (Fig. 3c). The smoothness of surface was further improved after the incorporation of wood, clay and SiO_2. The surface smoothness was increased up to the addition of clay (3 wt%) and SiO_2 (3 wt%) (Fig. 3d–e). The surface of WPC loaded with 5 wt% SiO_2 and clay (Fig. 3f) appeared less smoother compared to WPC loaded with 3 wt% SiO_2 and clay. The increase in smoothness might be due to the improvement in interaction among PE-*co*-GMA, hydroxyl groups of wood and clay, organic surfactant present in clay and polymer. Moreover, CTAB-modified SiO_2 also has long olefinic chain which further improved the interaction among them. The agglomeration occurred at higher percentage of SiO_2 loading might be due to the surface interaction between SiO_2 nanoparticles. Similar agglomeration of SiO_2 nanoparticles at higher percent of loading was observed by Chrissafis et al. [21] during the thermal study of HDPE/fumed silica nanocomposite.

FTIR results

FTIR spectra of CTAB, SiO_2, and CTAB-modified SiO_2 are shown in Fig. 4. The absorption peaks at 2,918, 2,848, and 1,475 cm^{-1} were assigned to asymmetric, symmetric, and scissor modes of $–CH_2$ stretching of the CTAB (curve a), respectively [22]. The spectrum of unmodified SiO_2 shows some absorption peaks at 3,424 for –OH stretching and 1,632 cm^{-1} for –OH bending of hydroxyl group adsorbed on surface of the particles. The other peaks appeared in the range 1,087–465 cm^{-1} were due to Si–O–Si group in the SiO_2 [23]. In the spectrum of CTAB-modified SiO_2,

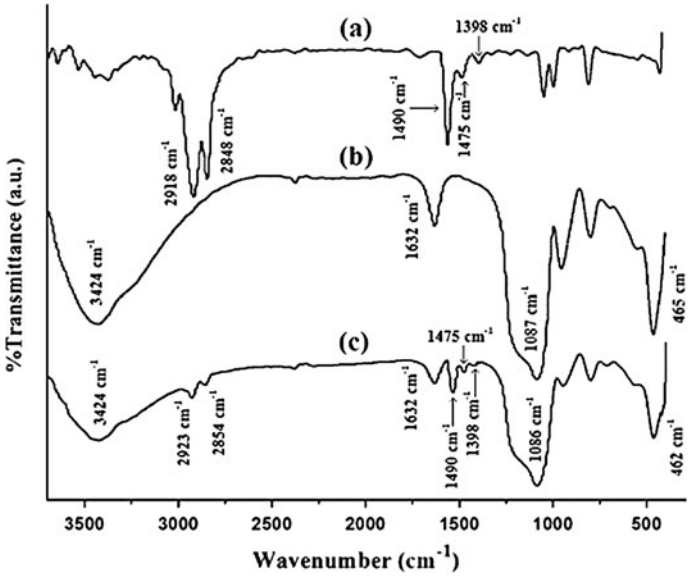

Fig. 4 FTIR spectra of (*a*) CTAB, (*b*) unmodified SiO_2, and (*c*) CTAB-modified SiO_2

the –OH peak intensity was found to decrease. This indicated an interaction of the hydroxyl group absorbed on SiO_2 surface with CTAB. Two new peaks at 2,923 and 2,854 cm^{-1} assigned for $–CH_2$ stretching of CTAB were also observed. The peaks at 1,490 and 1,398 cm^{-1} were due to the asymmetric and symmetric $CH_3–N^+$ deformation mode of CTAB headgroup [22]. Fu and co-workers [24] modified TiO_2 with CTAB and reported that the interaction of TiO_2 occurred with Br^- of CTAB through hydrogen bond formation or electrostatic attractions. The other notable peaks appeared in the CTAB-modified SiO_2 spectrum were the characteristic peaks for CTAB and SiO_2. These results indicated the incorporation of CTAB on the surface of SiO_2 particles.

Figure 5 shows the FTIR spectra of wood, nanoclay, PB/G5, WPC, and WPC loaded with nanoclay (3 wt%) and SiO_2 (1–5 wt%). Curve a shows the presence of absorption bands at 3,434 cm^{-1} for –OH stretching, 2,931 and 2,849 cm^{-1} for –CH stretching, 1,730 cm^{-1} for C=O stretching, 1,635 cm^{-1} for –OH bending, 1,163 and 1,045 cm^{-1} for C–O stretching and 1,000–645 cm^{-1} for C–H bending vibration (out of plane) of the wood sample. Organically modified nanoclay (curve b) exhibited the peaks at 3,470 cm^{-1} (–OH stretching) 2,935 and 2,849 cm^{-1} (–CH stretching of modified hydrocarbon), 1,620 cm^{-1} (–OH bending) and 1,030–460 cm^{-1} (oxide bands of metals like Si, Al, Mg, etc). Polymer blend loaded with compatibilizer (curve c) shows peaks at 2,919 and 2,838 cm^{-1} (–CH stretching), 1,473 cm^{-1} (–CH bending), and 714 cm^{-1} ($–CH_2$ bending). PB/G5/W40 (curve d) exhibited peaks at

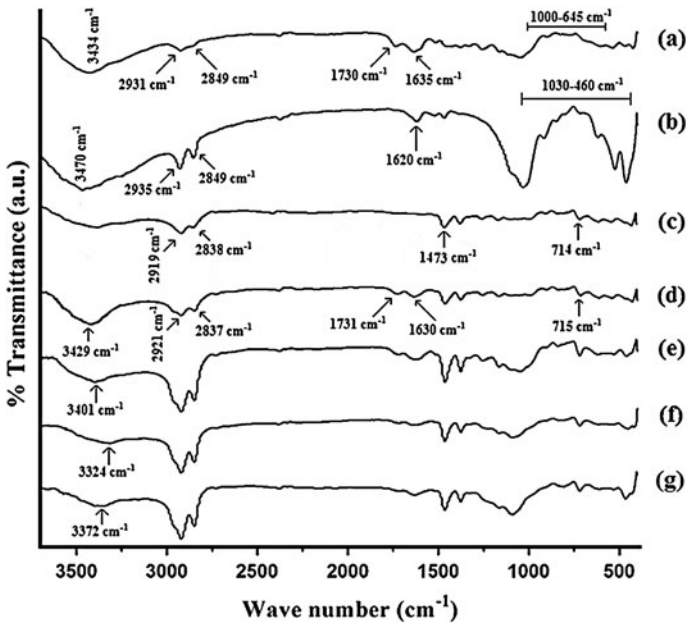

Fig. 5 FTIR spectra of (*a*) wood, (*b*) Nanoclay, (*c*) PB/G5, (*d*) PB/G5/W40, (*e*) PB/G5/W40/N3/S1, (*f*) PB/G5/W40/N3/S3, and (*g*) PB/G5/W40/N3/S5

3,429 cm^{-1} (–OH stretching), 2,921 and 2,837 cm^{-1} (–CH stretching), 1,731 cm^{-1} (C=O stretching), 1,630 cm^{-1} (–OH bending), and 715 cm^{-1} ($–CH_2$ bending).

Figure 5e–g represents the FTIR spectra of WPC loaded with 3 wt% nanoclay and 1, 3, and 5 wt% of SiO_2, respectively. It was observed that the intensity of –OH stretching decreased and shifted to 3,401 cm^{-1} (curve e), 3,324 cm^{-1} (curve f) and 3,372 cm^{-1} (curve–g) from 3,434 cm^{-1} (wood) and 3,470 cm^{-1} (nanoclay). The decreased in intensities and shifting to lower wavenumber confirmed the bond formation between the hydroxyl groups of wood, nanoclay and SiO_2. Moreover, the increase in intensities of –CH stretching at 2,921 and 2,837 cm^{-1} (curve e–g) compared to those of wood indicated an interaction between polymer, wood and compatibilizer. Similar type of decrease in intensity of –OH absorption peak, a shifting to lower wavenumber and increase in –CH peak intensities was reported by Maji and Deka [25]. In the spectra of WPC (curve e–g), the intensity of the metal oxides bond appeared in the range 1,030–460 cm^{-1}, corresponding to nanoclay and SiO_2, decreased to a desirable extent indicating the formation of bond between wood, clay, SiO_2, and polymers.

Mechanical property results

Table 1 shows the flexural and tensile properties of polymer blend, WPC and WPC loaded with nanoclay and different percentage of SiO_2 nanopowder. After incorporation of compatibilizer, both flexural and tensile properties of the polymer blend increased. This was because of the improvement in interfacial adhesion between the polymers by the compatibilizer. The values were further improved after the addition of WF. The improvements in flexural and tensile properties were due to the reinforcing action provided by WF. Moreover, the compatibilizer, PE-*co*-GMA, increased the interfacial adhesion between wood and polymers by its glycidyl linkage and long olefinic chain and thus improved the strength properties. Deka and Maji [26] studied the properties of polymer blend/WF composite and observed an

Table 1 Flexural, tensile and Hardness properties of polymer blend and WPC loaded with different percentage of nanoclay and SiO_2

Sample	Flexural properties		Tensile properties		Hardness
	Strength (MPa)	Modulus (MPa)	Strength (MPa)	Modulus (MPa)	(Shore D)
PB	13.47 ± 0.94	759.63 ± 1.06	5.73 ± 1.04	84.72 ± 16.37	66.6 (± 0.5)
PB/G5	16.25 ± 1.13	1031.19 ± 1.11	8.96 ± 1.26	115.51 ± 16.76	68.7 (± 0.3)
PB/G5/W40	18.14 ± 1.21	3798.72 ± 1.07	17.82 ± 1.15	263.42 ± 18.03	66.3 (± 0.7)
PB/G5/W40/N3/S1	30.52 ± 1.03	4971.60 ± 1.12	35.63 ± 1.17	636.41 ± 17.83	79.2 (± 0.1)
PB/G5/W40/N3/S3	37.26 ± 1.09	5686.91 ± 1.18	40.15 ± 1.26	692.75 ± 18.53	84.3 (± 0.6)
PB/G5/W40/N3/S5	32.53 ± 1.12	5172.50 ± 1.16	36.97 ± 1.12	647.53 ± 18.32	81.4 (± 0.2)

improvement in mechanical properties after the incorporation of compatibilizer and WF. The properties were further improved after the incorporation of clay and SiO_2. The silicate layers of nanoclay act as a reinforcing agent that binds the polymer chain inside the gallery space and thus restricts the mobility of the polymer chains. The increased in mechanical properties of wood–plastic composite after the incorporation of nanoclay was reported by Faruk and Matuana [27]. At a fixed level of nanoclay (3 wt%) loading, both flexural and tensile properties were improved up to the addition of 3 wt% SiO_2, beyond that level of SiO_2 loading, these values decreased. The surface hydroxyl groups of CTAB-modified SiO_2 nanopowder might interact with the hydroxyl groups of wood, while the long alkyl chain of CTAB could interact with the polymer blend. Hence, a well distribution of the nanoparticles occurred which increased the flexural and tensile properties of the composite. Yu et al. [28] reported that the mechanical properties of polyacrylonitrile improved due to addition of Na-MMT and SiO_2 nanopowder. At higher percentage of SiO_2 loading (5 wt%), the agglomeration of the nanoparticles resulted in a decrease in mechanical properties.

Hardness results

Hardness results of polymer blend and WPC with clay and different percentage of SiO_2 loading are also shown in Table 1. It was observed that after the incorporation of compatibilizer, hardness value of the polymer blend increased. The compatibilizer improved the interfacial adhesion between the polymers and hence increased the hardness value. After the addition of WF to the polymer blend, the value was found to decrease. But the hardness value was found to increase again after the incorporation of nanoclay and SiO_2 to the WPC. The improvement was due to the restriction in the mobility of the polymer chains provided by the silicate layers and increase in interaction between clay, SiO_2 nanopowder, wood, and polymer blend as mentioned earlier. At higher SiO_2 (5 wt%) loading, hardness value was found to decrease. The decrease in hardness value was due to the agglomeration of SiO_2 nanoparticles.

Thermal property results

Table 2 represents the initial decomposition temperature (T_i), maximum pyrolysis temperature (T_m), decomposition temperature at different weight loss (%) (T_D) and residual weight (RW, %) for the polymer blend and WPCs. The incorporation of compatibilizer and WF enhanced the T_i values of the polymer blend. The compatibilizer increased the interfacial adhesion among the polymers and with WF through its long hydrocarbon chain and glycidyl group that leads to an increase in the T_i values. Deka and Maji [26] observed an increase in thermal stability of polymer blend after incorporation of compatibilizer and WF. T_i value was further improved after the incorporation of clay and SiO_2 nanopowder. The tortuous path provided by the well distributed silicate layers of clay prevented the passage of volatile decomposed product throughout the composite. The incorporation of nanoclay improved the thermal stability of PP/WF nanocomposite [29]. The higher

Table 2 Thermal analysis and limiting oxygen index (LOI) values of polymer blend and wood polymer nanocomposite

Sample	T_i	T_m^a	T_m^b	Temperature of decomposition (T_D) in °C at different weight loss (%)				RW % at 600 °C	Limiting oxygen index (%)
				20 %	40 %	60 %	80 %		
PB	248	267	401	287	386	435	467	5.7	22
PB/G5	251	270	407	291	389	439	470	6.2	35
PB/G5/W40	256	278	448	299	402	447	477	7.1	38
PB/G5/W40/N3/S1	272	321	497	324	453	479	495	11.1	63
PB/G5/W40/N3/S3	278	329	503	335	461	484	501	14.0	68
PB/G5/W40/N3/S5	275	325	501	328	457	481	498	12.2	65

T_i value for initial degradation

[a] T_m value for 1st step

[b] T_m value for 2nd step

thermal diffusivity of SiO_2 nanoparticles improved the heat dispersion inside the composite. This would lead to a delay in burning of the surface and release of combustible volatile product throughout the composite. The incorporation of silica improved the thermal stability of PMMA [14]. At higher percentage (5 wt%) of SiO_2 loading, the agglomeration of oxide nanoparticles offered the passage of volatile products easily. Hence, the thermal stability decreased.

Limiting oxygen index (LOI) results

Table 2 also shows the LOI values of polymer blend, WPC and WPC loaded with nanoclay and SiO_2. It was observed that LOI value of the polymer blend increased after the addition of compatibilizer. The compatibilizer improved the interfacial adhesion among the polymers and thus increased in LOI value. LOI value was further increased after the incorporation of WF. A substantial improvement in LOI value was observed after the addition of clay and SiO_2. The value increased up to the addition of 3 wt% each of nanoclay and SiO_2, beyond that it decreased. The tortuous path provided by the silicate layers had better barrier property to the oxygen and heat which delayed the burning capacity of the composite. Guo et al. [30] observed that the flame retardancy of wood fiber–plastic composite increased after the incorporation of nanoclay. The addition of CTAB-modified SiO_2 enhanced the interaction between wood, clay, and polymer through its hydroxyl and cetyl groups. SiO_2 nanoparticles also provided some thermal barrier to the oxygen and heat leading to an improvement in flame retardant property. The improvement in flame retardancy of PP filament due to the inclusion of nano SiO_2 was reported by Erdem et al. [31]. At higher concentration of SiO_2 (5 wt%), LOI value decreased.

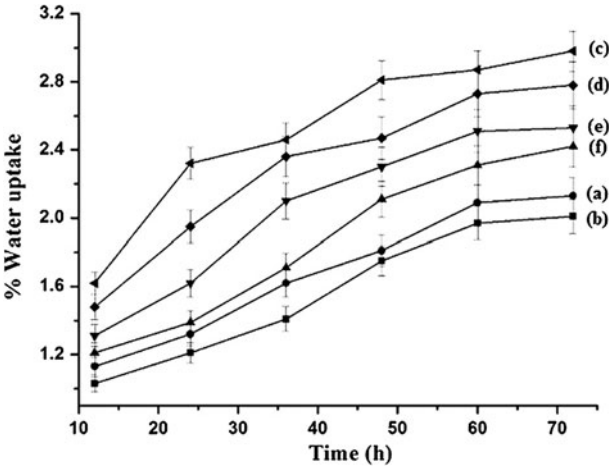

Fig. 6 Water uptake of (*a*) PB, (*b*) PB/G5, (*c*) PB/G5/W40, (*d*) PB/G5/W40/N3/S1, (*e*) PB/G5/W40/N3/S5, and (*f*) PB/G5/W40/N3/S3

The agglomeration of SiO_2 nanoparticles resulted in the decrease of interaction and hence reduction in barrier property as well as LOI value.

Water uptake results

The water uptake results of polymer blend, PE-*co*-GMA treated polymer blend and WPC loaded with clay and different percentage of SiO_2 are shown in Fig. 6. On addition of PE-*co*-GMA compatibilizer, water uptake of the polymer blend decreased. This was due to the improvement in interaction between the polymers by the compatibilizer. The value of water uptake was found to increase after the addition of WF to the blend. The hydrophilic nature of WF caused an increase in the water uptake value. The water uptake decreased after the addition of clay and SiO_2. WPC loaded with 3 wt% each of clay and SiO_2 showed lowest water uptake followed by WPC with 3 wt% clay and 5 wt% SiO_2, and WPC with 3 wt% clay and 1 wt% SiO_2. The tortuous path provided by the silicate layers of clay increased the barrier property for water transport [32]. The barrier property provided by SiO_2 nanopowder might prevented the passage of water. The more the distribution of nanoparticles, the better was the barrier property. Minelli et al. [33] reported that the water uptake of polyvinyl alcohol decreased after the incorporation of SiO_2 nanopowder. At higher concentration of SiO_2 (5 wt%), the agglomeration of nanoparticles might be responsible for the increase in water uptake value.

Conclusions

Solution blending of HDPE, LDPE, PP, and PVC (1:1:1:0.5) was optimized as 70:30. Use of polyethylene-*co*-glycidyl methacrylate (PE-*co*-GMA) as

compatibilizer improved the compatibility among the polymers and WF as studied by SEM. XRD and TEM analysis showed the distribution of silicate layers of nanoclay and SiO_2 in the composite. Surface modification of SiO_2 nanoparticles by cationic surfactant CTAB and the interaction among wood, PE-*co*-GMA, SiO_2, and nanoclay were examined by FTIR. WPC loaded with nanoclay and SiO_2 showed a remarkable improvement in flame retardancy, mechanical properties, and thermal stability. The incorporation of nanoclay and SiO_2 nanoparticles decreased the water uptake value of WPC. WPC loaded with 3 wt% each of clay and SiO_2 exhibited maximum improvement in properties.

Acknowledgments The authors thank Council of Scientific and Industrial Research (CSIR)-New Delhi for their financial assistance (Grant number: 01(2287)/08/EMR-II).

References

1. Xu X, Jayaraman K, Morin C, Pecqueux N (2008) Life cycle assessment of wood-fibre-reinforced polypropylene composites. J Mater Process Technol 198:168–177
2. Ashori A (2008) Wood–plastic composites as promising green-composites for automotive industries! Bioresour Technol 99:4661–4667
3. Sui G, Fuqua MA, Ulven CA, Zhong WH (2009) A plant fiber reinforced polymer composite prepared by a twin-screw extruder. Bioresour Technol 100:1246–1251
4. Ding C, He H, Guo B, Jia D (2008) Structure and properties of polypropylene/clay nanocomposites compatibilized by solid-phase grafted polypropylene. Polym Compos 29:698–701
5. Minkova L, Peneva Y, Valcheva M, Filippi S, Pracella M, Anguillesi I, Magagnini P (2010) Morphology, microhardness, and flammability of compatibilized polyethylene/clay nanocomposites. Polym Eng Sci 50:1306–1314
6. Giannakas A, Xidas P, Triantafyllidis KS, Katsoulidis A, Ladavos A (2009) Preparation and characterization of polymer/organosilicate nanocomposites based on unmodified LDPE. J Appl Polym Sci 114:83–89
7. Awad WH, Beyer G, Benderly D, Ijdo WL, Songtipya P, Gasco MMJ, Manias E, Wilkie CA (2009) Material properties of nanoclay PVC composites. Polymer 50:1857–1867
8. Selke SE, Wichman I (2004) Wood fiber/polyolefin composites. Compos A 35:321–326
9. Qiu W, Zhang F, Endo T, Hirotsu T (2005) Effect of maleated polypropylene on the performance of polypropylene/cellulose composite. Polym Compos 26:448–453
10. Devi RR, Maji TK (2007) Effect of glycidyl methacrylate on the physical properties of wood–polymer composites. Polym Compos 280:1–5
11. Song GJ (1996) Polymeric nano-metered composites. Mater Rep 4:57–60
12. Wu C, Xu T, Yang W (2005) Synthesis and characterizations of novel, positively charged poly (methyl acrylate)–SiO_2 nanocomposites. Eur Polym J 41:1901–1908
13. Zheng Y, Zheng Y, Ning R (2003) Effects of nanoparticles SiO_2 on the performance of nanocomposites. Mater Lett 57:2940–2944
14. Hu YH, Chen CY, Wang CC (2004) Viscoelastic properties and thermal degradation kinetics of silica/PMMA nanocomposites. Polym Degrad Stab 84:545–553
15. Mina F, Seema S, Matin R, Rahaman J, Sarker RB, Gafur A, Bhuiyan AH (2009) Improved performance of isotactic polypropylene/titanium dioxide composites: effect of processing conditions and filler content. Polym Degrad Stab 94:183–188
16. Han G, Lei Y, Wu Q, Kojima Y (2008) Bamboo-fiber filled high density polyethylene composites: effect of coupling treatment and nanoclay. J Polym Environ 16:123–130
17. Liu J, Chen G, Yang J (2008) Preparation and characterization of poly(vinyl chloride)/layered double hydroxide nanocomposites with enhanced thermal stability. Polymer 49:3923–3927
18. De Rosa C, Corradini P (1993) Crystal structure of syndiotactic polypropylene. Macromolecules 26:5711–5718
19. Bao Y, Ma JZ (2011) Polymethacrylic acid/Na-montmorillonite/SiO_2 nanoparticle composites structures and thermal properties. Polym Bull 66:541–549

20. Pracella M, Chionna D, Ishak R, Galeski A (2004) Recycling of PET and polyolefin based packaging materials by reactive blending. Polym Plast Technol Eng 43:1711–1722
21. Chrissafis K, Paraskevopoulos KM, Pavlidou E, Bikiaris D (2009) Thermal degradation mechanism of HDPE nanocomposites containing fumed silica nanoparticles. Thermochim Acta 485:65–71
22. Li H, Tripp CP (2002) Spectroscopic Identification and dynamics of adsorbed cetyltrimethylammonium bromide structures on TiO_2 surfaces. Langmuir 18:9441–9446
23. Kang JS, Yu CL, Zhang FA (2009) Effect of silane modified SiO_2 particles on poly(MMA-HEMA) soap-free emulsion polymerization. Iran Polym J 18:927–935
24. Qu Y, Wang W, Jing L, Song S, Shi X, Xue L, Fu H (2010) Surface modification of nanocrystalline anatase with CTAB in the acidic condition and its effects on photocatalytic activity and preferential growth of TiO_2. Appl Surf Sci 257:151–156
25. Deka BK, Maji TK (2010) Effect of coupling agent and nanoclay on properties of HDPE, LDPE, PP, PVC blend and *Phargamites karka* nanocomposite. Compos Sci Technol 70:1755–1761
26. Deka BK, Maji TK (2011) Study on the properties of nanocomposite based on high density polyethylene, polypropylene, polyvinyl chloride and wood. Compos A 42:686–693
27. Faruk O, Matuana LM (2008) Nanoclay reinforced HDPE as a matrix for wood–plastic composites. Compos Sci Technol 68:2073–2077
28. Yu T, Lin J, Xu J, Chen T, Lin S, Tian X (2007) Novel polyacrylonitrile/Na-MMT/silica nanocomposite: co-incorporation of two different form nano materials into polymer matrix. Compos Sci Technol 67:3219–3225
29. Nourbakhsh A, Ashori A, Tabari HZ, Rezaei F (2010) Mechanical and thermo-chemical properties of wood-flour/polypropylene blends. Polym Bull 65:691–700
30. Guo G, Park CB, Lee YH, Kim YH, Sain M (2007) Flame retarding effects of nanoclay on wood-fiber composites. Polym Eng Sci 47:330–336
31. Erdem N, Cireli AA, Erdogan UH (2009) Flame retardancy behaviors and structural properties of polypropylene/nano-SiO_2 composite textile filaments. J Appl Polym Sci 111:2085–2091
32. Yeh SK, Gupta RK (2010) Nanoclay-reinforced polypropylene-based wood–plastic composites. Polym Eng Sci 50:2013–2020
33. Minelli M, Angelis MGD, Doghieri F, Rocchetti M, Montenero A (2010) Barrier properties of organic–inorganic hybrid coatings based on polyvinyl alcohol with improved water resistance. Polym Eng Sci 50:144–153